Vectashield quenches Alexa Fluor 647 fluorescence, but does not hinder dSTORM super-resolution imaging

Aleksandra Arsić[1#], Nevena Stajković[1#], Rainer Spiegel[2], Ivana Nikić-Spiegel[1*]

[1]Werner Reichardt Centre for Integrative Neuroscience, University of Tübingen, Germany

[2]BG Hospital Tübingen, University of Tübingen, Germany

[#] equal contribution

[*]correspondence should be addressed to: Ivana Nikić-Spiegel, ivana.nikic@cin.uni-tuebingen.de

Abstract

The right choice of mounting medium is crucial for optimal microscopy. Different techniques require different mounting media. It was recently reported that Vectashield, one of the most commonly used media for conventional fluorescence microscopy, can also be used for super-resolution dSTORM (direct stochastic optical reconstruction microscopy) imaging of Alexa Fluor 647 (AF647). This is important because dSTORM usually requires self-made imaging buffers. As self-made buffers can introduce a lot of variation, using an off-the-shelf commercial imaging medium, such as Vectashield, brings more reproducibility. However, while testing its compatibility with dSTORM imaging of neurofilament light chain (NfL), we noticed an unexpected loss of AF647 fluorescence in Vectashield. We saw almost completely dark images and we thought that our immunolabeling did not work. However, as we discovered, dark AF647 samples have nothing to do with failed immunolabelings. Instead, the AF647 dye molecules are simply quenched. Initial intensity measured in Phosphate Buffered Saline (PBS) drops to about 15% in Vectashield. This loss of fluorescence means that Vectashield is not compatible with conventional fluorescence microscopy of AF647. However, although we can hardly recognize labeled cells in conventional microscopy, we can still perform 3D dSTORM super-resolution microscopy in these quenched, dark cells.

Introduction

Super-resolution microscopy (SRM) requires bright, densely labeled samples. Typical experiments start with dyes in a fluorescent state. This is necessary for the identification of labeled cells. A subsequent requirement for one type of SRM, dSTORM (direct stochastic optical reconstruction microscopy), is to get dye molecules to blink. Blinking separates individual fluorescent molecules in time and space. This enables their precise localization, which is necessary to reconstruct super-resolution diffraction-unlimited images[1,2]. In order to make them blink, dye molecules are switched to a dark state from which they stochastically and spontaneously recover to a fluorescent state, multiple times before bleaching. This can be achieved by special chemicals, such as thiol-containing reducing agents with or without enzymatic oxygen scavenger systems (e.g. GLOX buffer containing glucose oxidase and catalase)[3,4]. It was recently reported that Vectashield, a commercial mounting medium, can also be used for dSTORM imaging of certain dyes, such as Alexa Fluor 647 (AF647)[5]. This finding has high practical implications since AF647 is the most widely used dye for dSTORM and Vectashield is one of the most commonly used commercial mounting media.

Results and discussion

In comparison with self-made buffers, commercially available Vectashield represents a very convenient and affordable choice for dSTORM imaging medium. The fact that it can be used off-the-shelfis especially important for demanding techniques such as dSTORM. Using the same imaging medium brings more reproducibility and allows for more comparable results within and between different laboratories. However, when we tried to use it for the imaging of neurofilament light chain (NfL), we noticed an unexpected loss of AF647 fluorescence in Vectashield compared to phosphate-buffered saline (PBS) (Fig. 1a, Supplementary Fig. 1). This is specific to AF647, as we do not see it with Alexa Fluor 488 (AF488; Fig. 1b, Supplementary Fig. 1). It is also independent of the applied microscopy technique since we see it with confocal microscopy as well (data not shown). To quantify observed fluorescence intensity changes we transfected the cells with a plasmid containing nuclear

53 localization sequence (NLS)-mCherry fusion protein (Fig. 2a). We chose to use NLS-mCherry for
54 intensity measurements for multiple reasons. Firstly, it is uniformly distributed within the nucleus,
55 and can be easily labeled with the same primary antibody, followed by either AF488- or AF647-
56 conjugated secondary antibody. Additionally, mCherry gives a bright fluorescent signal in 561
57 channel that is not affected by any of the imaging media. This can be used for reliable identification
58 of labeled regions of interest and intensity measurements of AF647 and AF488 before and after
59 imaging media change (Fig. 2b; Supplementary Fig. 2; see material and methods for image acquisition
60 and analysis details). A quantitative analysis shows there is an intensity drop to about 15 % of the
61 initial value for AF647, and no loss of intensity for AF488 (Fig. 2d). Albeit not quantified before, this is
62 in accordance with previously published work suggesting that Vectashield is not optimal for storing of
63 AF647-labeled samples[6]. We first thought that our immunocytochemistry labeling with primary and
64 secondary antibodies might not be stable. That is why we tested different types of AF647 stainings.
65 We observed that the loss of fluorescence is not specific to our AF647-conjugated secondary
66 antibody. We also see it for the cells labeled with an AF647-conjugated primary antibody (Fig. 3) or
67 AF647-phalloidin (Supplementary Fig. 3). However, AF647 quenching is more or less noticeable when
68 looking at different cellular structures, probably depending on the starting labeling intensity. For
69 example, tubulin immunocytochemistry still shows relatively nicely labeled cells in Vectashield (Fig.
70 3a). Without seeing the image in PBS (before the addition of Vectashield), one might not even realize
71 that there was quenching. That might be a reason why the AF647 quenching has not been reported
72 before. On the other hand, even when we adjusted the image display (brightness/contrast) to show
73 very dim pixel values (auto scale lookup table; Fig. 1c, inset), NfL shows hardly any signal and the
74 labeling quality seems to be very poor. However, to our surprise, even with such “dark” NfL samples,
75 it is still possible to do dSTORM. Although we can hardly identify positively labeled cells in
76 Vectashield, we can still see blinking, perform 3D dSTORM imaging and even obtain SRM images with
77 a resolution of less than 40 nm (Fig. 1c), as estimated by Fourier ring correlation[7]. However, this was
78 only made possible by identifying the labeled cell in PBS before adding Vectashield, i.e. before the

image turned dark. Otherwise, it is not possible to tell apart background from a labeled cell. In addition to checking the cells in PBS first, and then switching to Vectashield for dSTORM, an alternative would be to use 25% Vectashield (Fig. 2d). It was previously reported that using 25% Vectashield in Tris-glycerol helps with reducing Vectashield's autofluorescent background[5]. Our quantitative analysis shows that 25% Vectashield does not induce quenching of AF647, similar to GLOX (Fig. 2d). In the context of SRM imaging, this is very important, since it not only allows us to identify labeled cells, but also to evaluate the labeling quality, which is a prerequisite for successful dSTORM. While trying to understand the mechanism behind the quenching, we came across reports on Vectashield inducing cleavage of cyanine dyes and their derivatives (especially Cy2). We thought that this might be happening with AF647. We tested this hypothesis in a recovery experiment where we washed away Vectashield and after some time imaged the cells again in PBS. A quantitative analysis shows that the loss of AF647 is reversible since it can be partially recovered (Fig. 2c, d; see material and methods for analysis details). The recovery would not have been possible if the dye was cleaved. In summary, we show that Vectashield induces quenching of AF647. On the contrary, AF488 fluorescence is increased in both pure and 25% Vectashield (respectively to 125 % and 185 % of the initial PBS values). Our findings have important consequences for any type of fluorescence microscopy. AF647 in Vectashield is not compatible with conventional fluorescence microscopy, because it gets quenched. This is especially of relevance for immunohistochemical stainings since Vectashield is used very commonly to mount tissue sections. Surprisingly, Vectashield-induced quenching does not hinder at least one type of microscopy, i.e. dSTORM. However, without knowing this, non-labeled and quenched cells cannot be distinguished. This would result in scientists not even trying to perform dSTORM, which would be wrong, considering the high quality of dSTORM images that can be achieved with Vectashield. Even though we only looked at AF647 and AF488 in this manuscript, similar changes might be happening with other fluorophores, other mounting media or other dSTORM imaging buffers. That is why for any type of labeling, we would recommend to always first check the cells in buffers such as PBS. That is the only way to distinguish between failed

105 immunocytochemistry/immunohistochemistry stainings and unexpected fluorescence quenching

106 phenomena.

107 # Figures

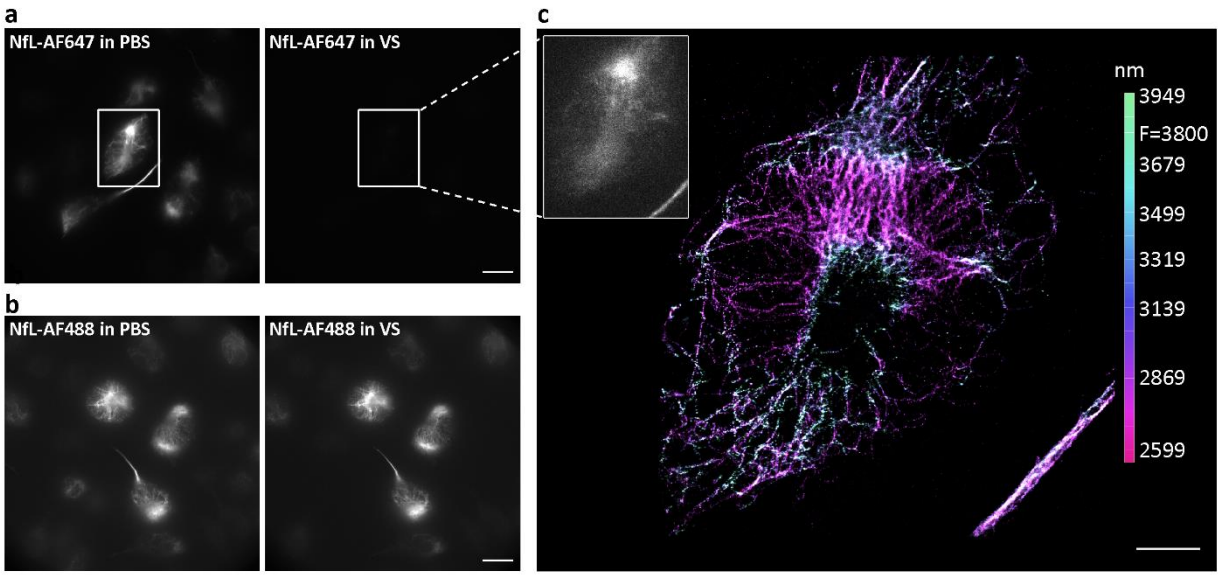

108
109 **Figure 1.** Vectashield (VS) quenches AF647 fluorescence, but does not hinder dSTORM super-resolution imaging.
110 ND7/23 cells were labeled with anti-NfL antibody, followed by AF647-(a,c) or AF488-conjugated secondary
111 antibody (b). Cells were first imaged with widefield illumination in PBS (a-b, left), then in Vectashield (a-b, right).
112 After replacing PBS with Vectashield, there is a significant drop in AF647 fluorescence intensity. Boxed regions
113 (a) show the location of the same cell. Brightness and contrast are linearly adjusted to show the same display
114 range, so that the effects of two imaging media can be compared. Even with 647 laser illumination and auto
115 scale look up table (c, inset), one can hardly recognize the original cell. However, despite AF647 being quenched,
116 the cell can still be successfully imaged with 3D dSTORM (c). The z positions in the 3D dSTORM image are color-
117 coded according to the height map shown on right. In contrast to AF647, after replacing PBS with Vectashield,
118 there is no change in AF488 fluorescence intensity (b). Scale bars: 20 µm (a,b), 5 µm (c).

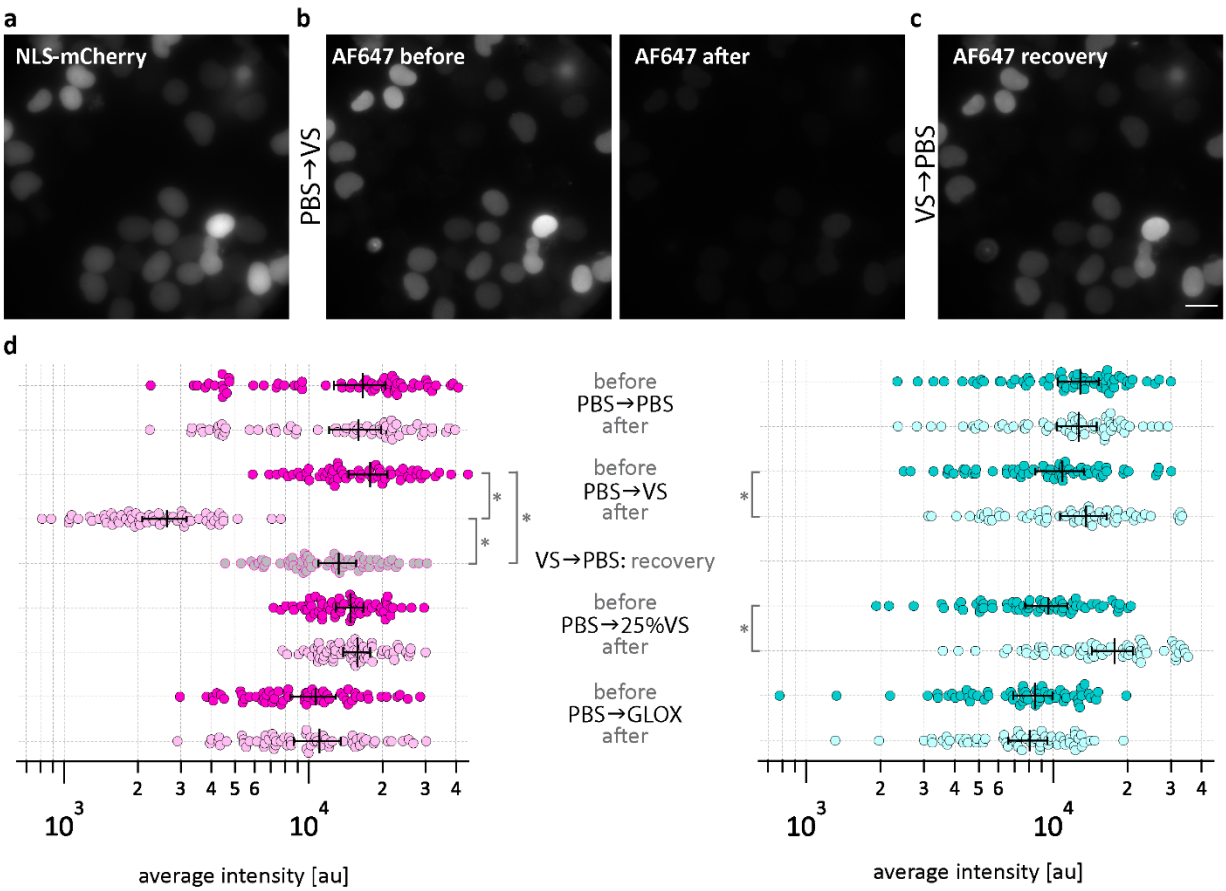

Figure 2. Quantification of intensity changes for AF647 and AF488 in different imaging media. Quantification was done on ND7/23 cells expressing NLS-mCherry (a) and labeled with anti-tRFP primary antibody, followed by AF647- or AF488- conjugated secondary antibody. Example images for AF647 are shown in a-c. Cells were first imaged in PBS, then in Vectashield (PBS→VS, b). Afterwards, Vectashield was replaced with PBS, cells were washed and imaged 2.5 h later in PBS (VS→PBS, c). After medium change from PBS to Vectashield (AF647 after), there is a significant drop in the AF647 fluorescence intensity that is partially recovered after washing (AF647 recovery). Additional examples for both AF647 and AF488 are shown in Supplementary Figure 2. Dot plots in panel d show results of intensity change quantification in different imaging media (PBS, VS, 25%VS, GLOX) for AF647 (magenta) and AF488 (cyan). In each case, cells were first imaged in PBS (before), followed by medium change (after). Average fluorescence intensity values of all images from 3 experiments (20 images per medium were analyzed in each experiment) are shown in the dot plot, including mean, and the standard error of the mean. Post-hoc Bonferroni comparisons (more details in material and methods) show that in all 3 experiments there is a significant decrease of AF647 intensity after changing the medium from PBS to Vectashield (PBS→VS; $p<0.05$), as well as significant increase after washing (VS→PBS: recovery; $p<0.05$). For AF488, there is a significant increase of intensity in VS and 25%VS (PBS→VS, $p<0.05$; PBS→25% VS, $p<0.05$). For

135 both AF488 and AF647 there is no significant intensity change after switching the imaging medium from PBS to
136 GLOX or in control condition (PBS to PBS media change). Average intensity (X-axis) is shown on a logarithmic
137 scale. Scale bar: 20 µm (a-c).

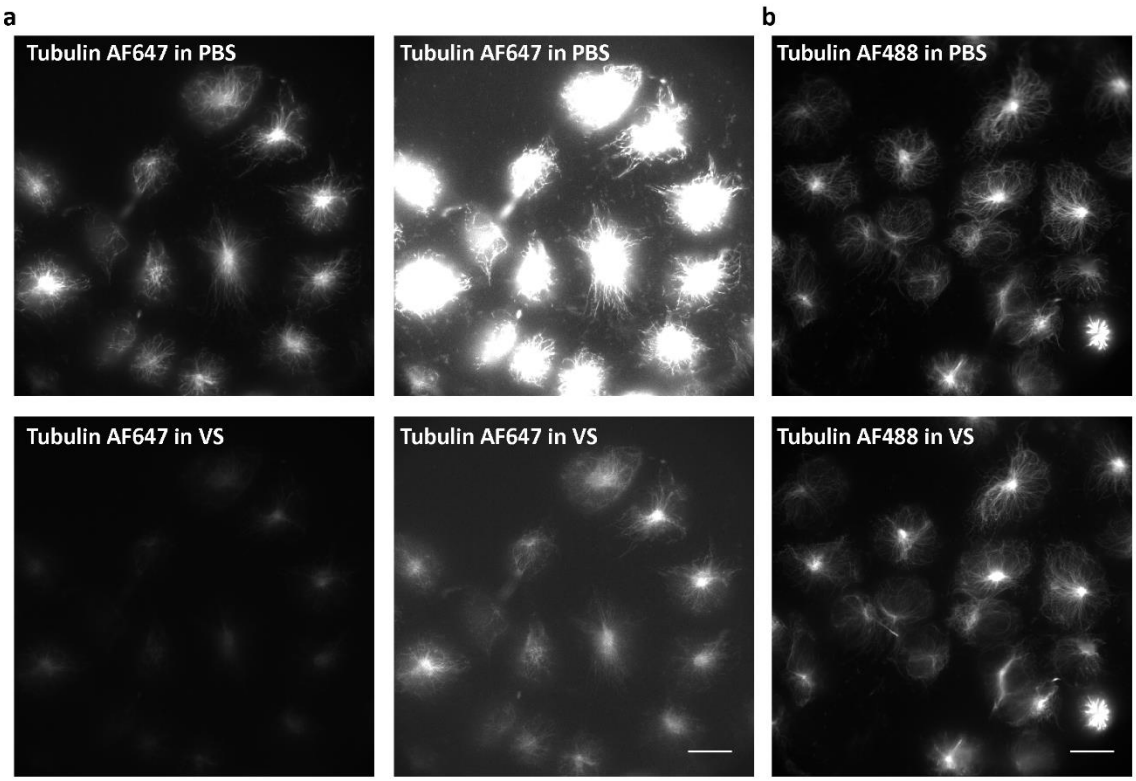

138
139 **Figure 3.** Vectashield effect on AF647- vs. AF488-labeled microtubules. ND7/23 cells labeled with AF647- (a) or
140 AF488-conjugated (b) anti-Tubulin β3 (TUBB3) antibody. Cells were first imaged in PBS (upper panels).
141 Afterwards, PBS was replaced with Vectashield (lower panels). As shown in the panel (a), after replacing PBS
142 with Vectashield, there is a drop in the AF647 fluorescence intensity. Please note that left and middle panels in
143 (a) show the same images for which brightness and contrast levels were adjusted differently in order to make
144 the quenched AF647 signal in Vectashield visible. In contrast to AF647, Vectashield does not quench AF488
145 fluorescence (b). Scale bar: 20 µm (a,b).

146

147 **Supplementary Figures**

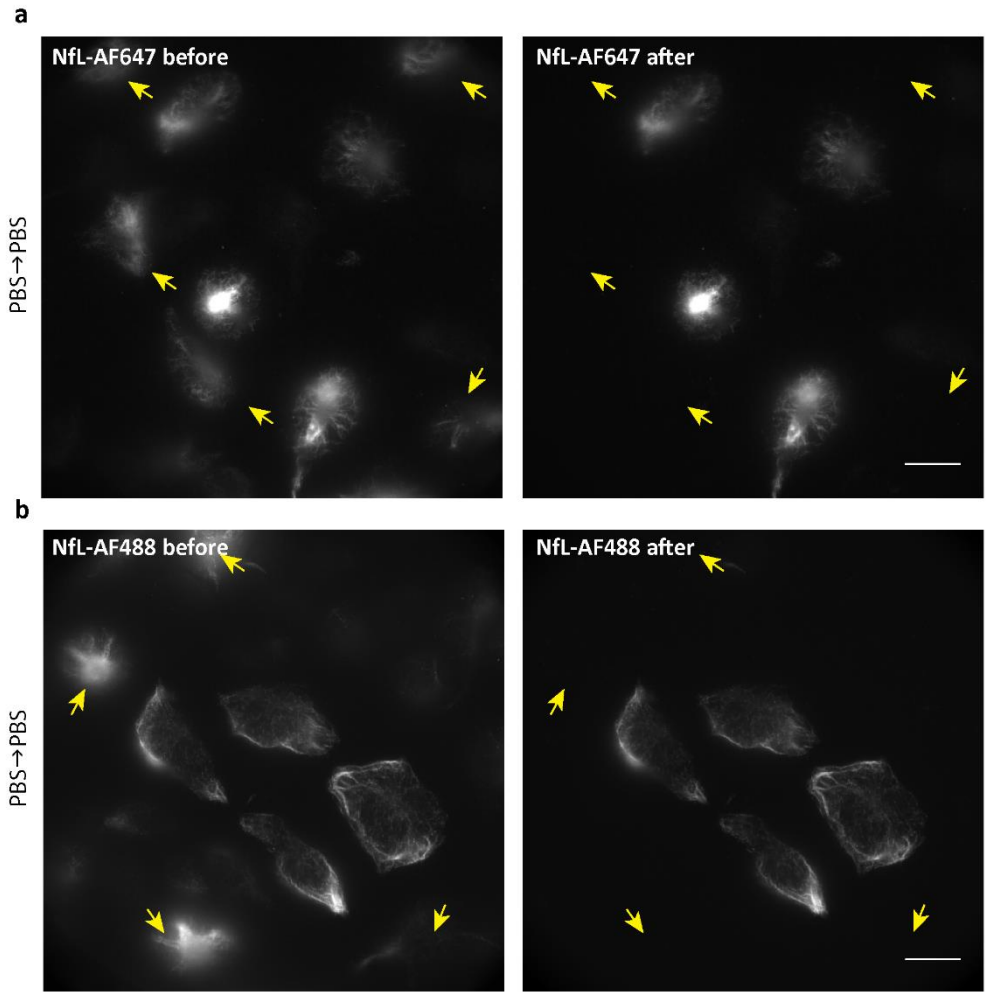

148
149 **Supplementary Figure 1.** Control experiments with PBS to PBS media change (PBS→PBS) show no effect on
150 fluorescence intensity of AF647- (a) and AF488- (b) labeled neurofilaments. ND7/23 cells labeled with anti-NfL
151 primary antibody, followed by AF647- or AF488-conjugated secondary antibody. Cells were first imaged in PBS
152 (left panels). Afterwards, PBS was replaced with PBS (right panels). In both cases, medium change does not
153 affect fluorescence intensity. Please note that some cells get washed away during medium change – they
154 cannot be identified in the image after medium change, and are marked with yellow arrows. In both a and b,
155 brightness and contrast are linearly adjusted to show the same display range for images taken before and after
156 media change. Scale bar: 20 µm (a,b).

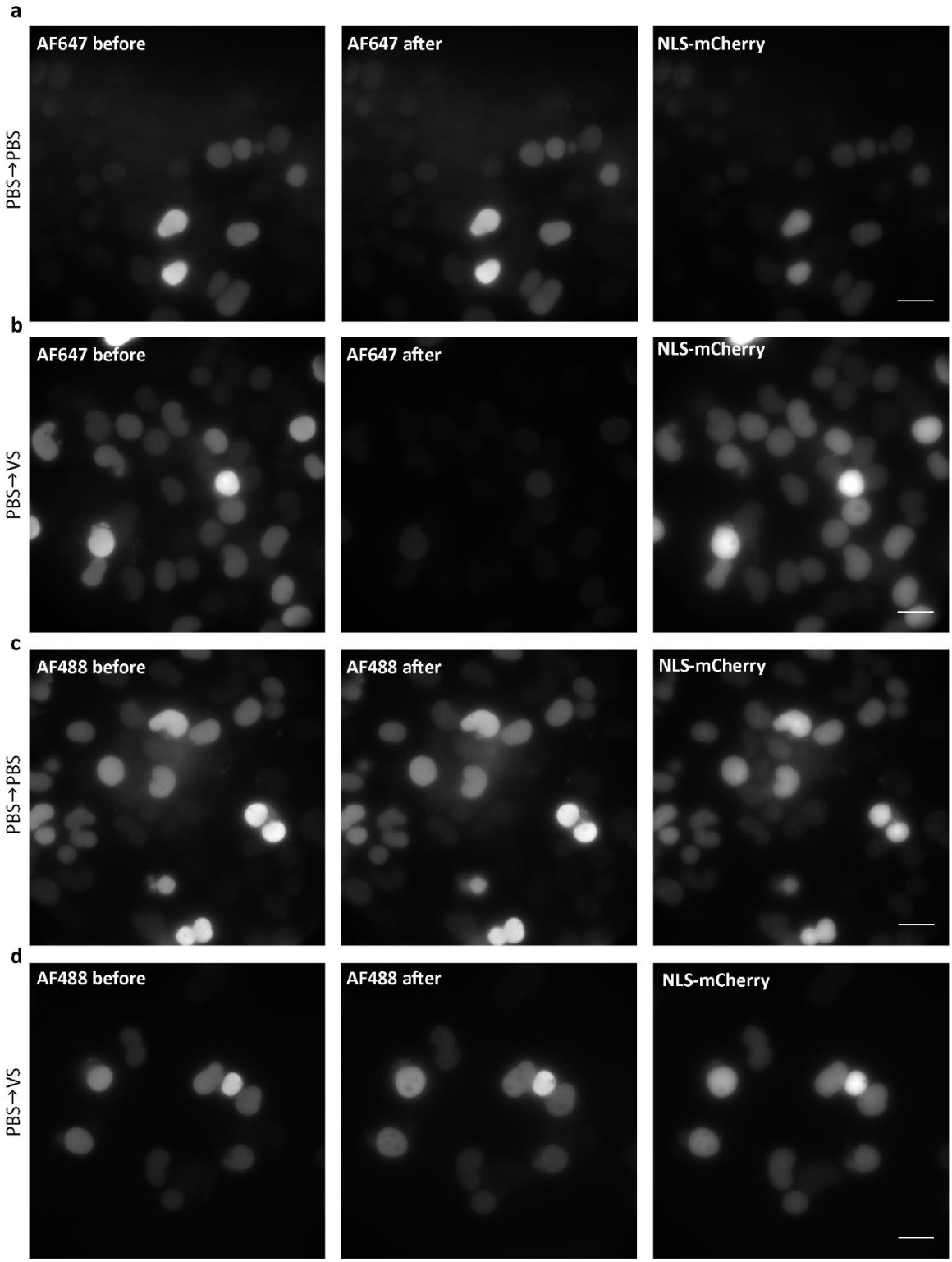

Supplementary Figure 2. Additional examples of images used for quantification of intensity changes for AF647 (a,b) and AF488 (c,d). As in Figure 2, cells were first imaged in PBS. Afterwards, PBS was replaced with PBS (PBS→PBS) or Vectashield (PBS→VS). Left panels show images before medium change and middle panels show images after medium change. In control condition (PBS→PBS, a) there is no difference in AF647 intensity, while in Vectashield (PBS→VS, b) there is a significant drop in the AF647 signal. In contrast to AF647, Vectashield

163 does not quench AF488 fluorescence (c,d). Right panels show corresponding mCherry channel images after

164 medium change. Scale bar: 20 µm (a-d).

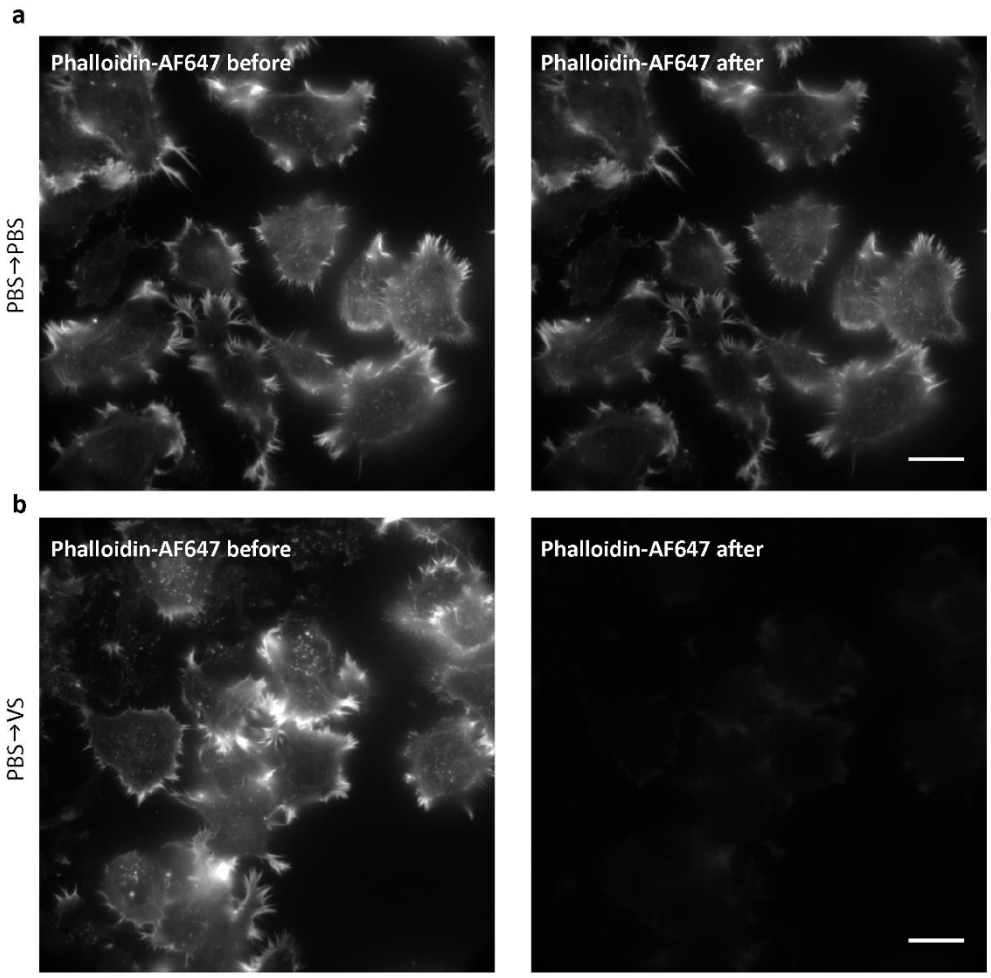

Supplementary Figure 3. Comparison of PBS vs. Vectashield effect on AF647-phalloidin. ND7/23 cells were labeled with AF647 phalloidin. Cells were first imaged in PBS. Afterwards, PBS was replaced with PBS (PBS→PBS, a) or Vectashield (PBS→VS, b). Left panels show images before medium change and right panels show images after medium change. In PBS (a) there is no difference in AF647 intensity, while in Vectashield (b) there is a drop in the AF647 signal. Scale bar: 20 µm (a,b).

171 # Material and Methods

172 **Cell culture**

173 Mouse neuroblastoma x rat neuron hybrid ND7/23 cells (ECACC 92090903, obtained from Sigma
174 Aldrich) were grown in high glucose Dulbecco's Modified Eagle Medium (DMEM; Thermo Fisher
175 Scientific, cat. no. 41965062) supplemented with 10 % heat-inactivated fetal bovine serum (FBS;
176 Thermo Fisher Scientific, cat. no. 10270106), 1 % penicillin-streptomycin (Sigma Aldrich, cat. no.
177 P0781), 1 % sodium pyruvate (Thermo Fisher Scientific, cat. no. 11360039) and 1 % L-glutamine
178 (Thermo Fisher Scientific, cat. no. 25030024) at 37 °C, 5 % CO_2. FBS was heat-inactivated by
179 incubation at 56 °C for 30 minutes. Cells were passaged every 2-3 days up to passage 18-20 and were
180 not differentiated.

181 For all the experiments, cells were seeded on a four-well Lab-Tek II chambered #1.5 German
182 coverglass (Thermo Fisher Scientific, cat. no. 155382), 70,000 cells per well. Lab-Teks were coated
183 with poly-D-lysine (Sigma Aldrich, cat. no. P6407) diluted in ddH2O at a 1 µg/ml concentration, and
184 incubated at least 4 h at room temperature (RT). Before seeding wells were washed twice with
185 Dulbecco's phosphate-buffered saline (DPBS; Thermo Fisher Scientific, cat. no. 14190169) or ddH_2O
186 and left in the hood to dry completely.

187 **Constructs and cloning**

188 NLS (nuclear localization sequence)-mCherry construct was made by inserting NLS-mCherry sequence
189 into a commercially available pcDNA^{TM}3.1/Zeo$^{(+)}$mammalian expression vector (Invitrogen). NLS
190 sequence was added upstream of the mCherry gene (gift from Edward Lemke's laboratory, EMBL,
191 Heidelberg) by polymerase chain reaction (PCR). The following primers were used for cloning: 5'-
192 GCTGGCGCTAGCACCATG**CCGCCGAAAAAAAAACGCAAAGTGGAAGATAGC**GTGAGCAAGGGCGAGGAGG
193 -3' (forward primer with NheI restriction site; NLS sequence is shown in bold) and 5'-

194 CGCGCAGCGGCCGCTCACTTGTACAGCTCGTCCATGCCG-3' (reverse primer with NotI restriction site).
195 Generated plasmid sequence was confirmed by sequencing.

196 **Transfections (for AF647 and AF488 intensity measurements)**

197 For Alexa Fluor 647 (AF647) and Alexa Fluor 488 (AF488) intensity measurement experiments,
198 ND7/23 cells were transfected with NLS-mCherry plasmid. Cells were transfected using JetPrime
199 (Polyplus-transfection, cat. no. 114-15) one day after seeding, at 80-85 % confluence, according to
200 the manufacturer´s instructions. On the following day, NLS-mCherry expression was confirmed on an
201 epifluorescent inverted microscope (Olympus CKX41) and immunostaining was started.

202 **Immunocytochemistry stainings**

203 For immunostaining of NLS-mCherry, cells were washed briefly with 0.01 M phosphate-buffered
204 saline (PBS; 137 mM NaCl, 10 mM Na_2HPO_4, 1.8 mM KH_2PO_4, 2.7 mM KCl, pH 7.4) and fixed with 2 %
205 paraformaldehyde (PFA; Sigma Aldrich, cat. no. 158127) in PBS for 10 min at RT. After fixation, cells
206 were briefly washed 3 times, blocked and permeabilized with 10 % goat serum (GS; Thermo Fisher
207 Scientific, cat. no. 16210064)/0.5 % Triton X-100/PBS (Sigma Aldrich, cat. no. X100) for 1 h. NLS-
208 mCherry was stained with rabbit anti-tRFP (turbo red fluorescent protein) antibody (Evrogene, cat.
209 no. AB233) diluted 1:500 in 5 % GS/0.1 % Triton X-100/PBS. The cells were incubated with primary
210 antibody at least 18 h at 4 °C. On the following day, cells were washed 3 times (5 minutes each wash)
211 and incubated with secondary goat anti-rabbit antibody conjugated with either AF647 (Thermo
212 Fisher Scientific, cat. no. A-21245) or AF488 (Thermo Fisher Scientific, cat. no. A-11034) for 1 h at RT.
213 Secondary antibodies were diluted 1:500 in 5 % GS/0.1 % Triton X-100/PBS. After incubation with the
214 secondary antibody, cells were washed 3 times (5 minutes each wash) and incubated in PBS until
215 imaging. All the washing steps were performed with PBS. Imaging was performed on the same or
216 following day.

217 For immunostaining of neurofilament light chain (NfL), cells were rinsed briefly with Tris-buffered
218 saline (TBS; 20 mM Tris, 150 mM NaCl, pH 7.6) and then fixed with 2 % PFA for 15 minutes at RT.

219 After fixation, cells were washed three times (5 minutes each wash) with TBS and blocked in
220 3 % GS/0.3 % Triton X-100/TBS for 40 minutes at RT. Cells were incubated with mouse anti-
221 neurofilament 70 kDa antibody, clone DA2 (Merck Millipore, cat. no. MAB1615) diluted 1:250 in
222 1 % GS/0.3 % Triton X-100/TBS for 2.5 h at RT, followed by overnight incubation at 4 °C. On the
223 following day, cells were washed 3 times (5 minutes each wash) with TBS, and incubated with goat
224 anti-mouse secondary antibodies conjugated with AF647 Plus (Thermo Fisher Scientific, cat. no.
225 A32728) or AF488 Plus (Thermo Fisher Scientific, cat. no. A32723) for 1 h at RT. Secondary antibodies
226 were diluted 1:500 in 1 % GS/0.3 % Triton X-100/TBS. Afterwards, cells were washed 3 times (5
227 minutes each wash) with TBS. TBS was used instead of PBS for this immunostaining because of
228 potential influence of PBS on phosphorylated neurofilaments. Only before imaging, TBS was replaced
229 with PBS. Imaging was performed on the same day.

230 For actin labeling with phalloidin AF647, cells were rinsed briefly with PBS and fixed with 2 % PFA, for
231 15 minutes at RT. After fixation, cells were washed 3 times briefly with PBS and blocked 1.5 h at RT in
232 5 % bovine serum albumin (BSA; Sigma Aldrich, cat. no. A9647) diluted in 0.3 % Triton X-100/PBS.
233 After blocking, cells were incubated with 0.25 µM AF647 phalloidin (Thermo Fisher Scientific, cat. no.
234 A22287) diluted in PBS, ON at 4 °C. On the following day, cells were incubated in AF647 phalloidin for
235 additional 4 h at RT and subsequently washed 3 times (5 minutes each wash) with PBS. Imaging was
236 performed on the same day.

237 For tubulin labeling cells were fixed as described previously[5]. Briefly, the cells were first washed with
238 PBS and extracted in 0.5 % Triton X-100 diluted in microtubule stabilization buffer (MTSB; 80 mM
239 PIPES, 1 mM $MgCl_2$, 5 mM EGTA, pH 6.8) for 10 seconds. Cells were washed once briefly with PBS,
240 and fixed in -20 °C methanol for 10 minutes at -20 °C. Afterwards, cells were washed 3 times (10
241 minutes each wash) and blocked for 1 h at RT in 5 % BSA/PBS. Cells were incubated with AF647 anti-
242 Tubulin β3 (TUBB3) antibody (BioLegend, cat. no. 801210) or AF488 anti-Tubulin β3 (TUBB3) antibody
243 (BioLegend, cat. no. 801203) diluted 1:100 in 5 % BSA/PBS, 3 h at RT. Afterwards, cells were washed

244 3 times (5 minutes each wash) with PBS and imaged on the same day. All washing, incubation and
245 blocking steps were performed on the shaker.

246 **Microscope configuration**

247 Widefield epifluorescence and 3D dSTORM imaging were performed on an N-STORM 4.0 microscope
248 from Nikon Instruments. More specifically, this is an inverted Nikon Eclipse Ti2-E microscope (Nikon
249 Instruments), equipped with XY-motorized stage, Perfect Focus System, an oil-immersion objective
250 (HP Apo TIRF 100×H, NA 1.49, Oil) and N-STORM module. Setup was controlled by NIS-Elements AR
251 software (Nikon Instruments). Fluorescent light was filtered through following filter cubes: 488 (AHF;
252 EX 482/18; DM R488; BA 525/45), 561 (AHF; EX 561/14; DM R561; BA 609/54) and Cy5 (AHF; EX
253 628/40; DM660; BA 692/40). Filtered emitted light was imaged with ORCA-Flash 4.0 sCMOS camera
254 (Hamamatsu Photonics). For epifluorescent widefield imaging, fluorescent lamp (Lumencor Sola SE II)
255 was used as a light source. For 3D dSTORM imaging of neurofilaments, 647 nm laser (LU-NV Series
256 Laser Unit) was used and cylindrical lens was introduced in the light path[8].

257 **Imaging of tRFP labeled cells (for AF647 and AF488 intensity measurements)**

258 tRFP labeled cells were first briefly checked in PBS using brightfield illumination. For each well in the
259 Lab-Tek we did following: picked randomly 30 fields of view (stage positions) using brightfield
260 illumination, saved xyz coordinates of each field of view in NIS-Elements AR software and acquired
261 images automatically by using NIS-Elements ND multipoint acquisition module, which allowed us to
262 go to the same position each time. The images were acquired in widefield mode, with 10 ms
263 exposure time, 1024x1024 pixels frame size and 16-bit image depth. To provide that the cells were
264 always properly focused, we used an autofocusing function of ND multipoint acquisition module.

265 Imaging was done first in PBS, using 561 (mCherry channel) and either 488 (AF488 channel) or Cy5
266 (AF647 channel) filter cube, depending on the labeling condition. Excitation light intensity for
267 mCherry and AF647 channels was 10 % and for AF488 channel 5 %. Afterwards, PBS was replaced
268 with one of the following imaging media: PBS, 100 % Vectashield (VS; Biozol, cat. no. VEC-H-1000),

269 25 % Vectashield or GLOX. We made 25 % Vectashield by mixing VS with Tris-Glycerol in 1:4 v/v ratio.
270 Tris-glycerol was obtained by adding 5 % v/v 1 M Tris, pH 8 to glycerol (Sigma Aldrich, cat.
271 no. G2025). For preparation of GLOX buffer, we used Buffer A (10 mM Tris, pH 8, 50 mM NaCl),
272 Buffer B (50 mM Tris, pH 8, 10 mM NaCl) and GLOX solution. GLOX solution was made by mixing 14
273 mg glucose oxidase (Sigma Aldrich, cat. no. G2133), 50 µl catalase (17 mg/ml; Sigma Aldrich, cat. no.
274 C3155) and 200 µl Buffer A. Aliquots of GLOX solution were kept at -20 °C. GLOX buffer was prepared
275 fresh, prior to use by mixing 7 µl GLOX solution with 690 µl Buffer B containing 10 % w/v glucose
276 (Sigma Aldrich, cat. no. D9559) on ice. For AF647 recovery experiments, 100 % Vectashield was
277 removed and cells were washed twice with PBS. After 2.5 h, cells were washed one more time with
278 PBS and imaging was repeated. To provide enough data for analysis each experiment was repeated
279 at least three times for AF488 labeled cells and AF647 labeled cells.

280 **Imaging of actin (phalloidin) and tubulin labeled cells**

281 Phalloidin AF647 labeled cells were first checked in PBS, using fluorescent light source (Lumencor
282 Sola SE II) and Cy5 filter cube with 10 ms exposure time and 5 % excitation light intensity. Up to 40
283 fields of view (positions) per well were picked and xyz coordinates of each field of view were saved in
284 NIS-Elements AR software. Widefield image acquisition was then performed automatically by using
285 NIS-Elements ND multipoint acquisition module at 30 ms exposure time and 10 % of fluorescent light
286 source. Both, brightfield and fluorescence images were acquired. Afterwards, PBS was replaced with
287 Vectashield, left 2 minutes to completely cover the sample and acquisition was repeated. Upon the
288 addition of Vectashield we noticed a change in focus, so before acquiring images in Vectashield,
289 every field of view needed to be manually refocused. During the imaging, autoscaling look-up table
290 (LUT) was on, which allowed us to see what would approximately be the correct focus plane, despite
291 the quenching of fluorescent signal.

292 Tubulin AF647 or AF488 labeled cells were imaged by following the same procedure as described
293 above, using Cy5 filter cube (AF647) or 488 filter cube (AF488).

294 **3D dSTORM imaging of NfL**

295 3D dSTORM (direct stochastic optical reconstruction microscopy) imaging was performed by using
296 the N-STORM module of Nikon microscope described above. For imaging, oil-immersion objective
297 (HP Apo TIRF 100×H, NA 1.49, Oil) and 647 nm laser (LU-NV Series Laser Unit) were used. Fluorescent
298 light was filtered through a Cy5 filter cube. Filtered emitted light was imaged with ORCA-Flash 4.0
299 sCMOS camera (Hamamatsu Photonics) with cylindrical lens introduced in the light path[8].

300 Fluorescent and brightfield images of NfL labeled cells in PBS and Vectashield were acquired
301 following the same procedure that was used for imaging of phalloidin AF647 labeled cells, using
302 fluorescent light source and Cy5 filter cube. After widefield acquisition, selected fields of view were
303 imaged with 3D dSTORM. Imaging was performed in total internal reflection fluorescence (TIRF) or
304 highly inclined and laminated sheet microscopy (HiLo) mode with continuous 647 nm laser
305 illumination (full power). Frame size was 256x256 pixels and image depth 16-bit. For each 3D
306 dSTORM image, 30,000 frames were acquired at 33 Hz.

307 Calibration of 3D dSTORM was done previously using TetraSpeck Microspheres (Thermo Fisher
308 Scientific, cat. no. T7279) following NIS-Elements' instructions. 3D dSTORM image processing was
309 performed in NIS-Elements AR software. Molecule identification settings were set to defaults for 3D
310 dSTORM analysis: minimum width 200 nm, maximum width 700 nm, initial fit width 300 nm, max
311 axial ratio 2.5 and max displacement 1. Minimum height for peak detection was set to 200, and
312 localization analysis was performed with overlapping peaks algorithm. Resulting molecule lists were
313 exported as text files and analyzed by Fourier ring correlation (FRC)[7] to determine the image
314 resolution. Based on FRC resolution estimate (35-40 nm), we reconstructed 3D dSTORM images with
315 Gaussian rendering size of 15 nm in NIS Elements AR. Brightness and contrast were adjusted with
316 Gaussian rendering intensity and height map with color coded molecule height (z location) was
317 added. Final 3D dSTORM image was then exported as a tiff image. Z rejected molecules were
318 excluded from resolution analysis and from final images.

319 **Image analysis and intensity measurements**

320 Intensity measurements for quantitative analysis of AF647 and AF488 were done in Fiji/ImageJ[9].
321 Images in ND2 format were opened using Bio-Formats plugin[10] and converted to tiff before the
322 analysis. Original bit depth (16-bit) was used for analysis. For presentation purposes, brightness and
323 contrast of 16-bit images were linearly adjusted in Fiji, images were converted to 8-bit and imported
324 in Adobe Illustrator.

325 In all of our experiments (except recovery of AF647) each field of view was imaged two times: in 561
326 (mCherry) and either 647 (AF647) or 488 (AF488) channel, before and after medium change. As
327 result, for each field of view we had four fluorescent pictures, mCherry and AF647(or AF488) before
328 and after medium change. In AF647 fluorescence recovery experiments each field of view was
329 imaged three times: in mCherry and AF647 channel, before medium change, after changing to
330 Vectashield and after washing in PBS. Consequently, for each field of view in recovery experiments
331 we had six fluorescent pictures, mCherry and AF647 before medium change, in Vectashield and after
332 washing in PBS.

333 For the purpose of analysis, we made a macro that allowed us to stack and align all images of each
334 field of view and perform the intensity measurements in same regions of interest (ROIs). Images from
335 mCherry channel were used for alignment and thresholding, while intensity measurements were
336 done in images from AF647 and AF488 channels, respectively.

337 Macro was designed to open and stack images from mCherry channel, align them using
338 MultiStackReg (developed by Brad Busse http://bradbusse.net/sciencedownloads.html) and
339 TurboReg plugin[11], and save the alignment information in a form of transformation matrices. After
340 that, macro was opening and stacking images from AF647 channel. AF647 images were aligned using
341 transformation matrices that were saved after alignment of mCherry images. This way we ensured
342 that images from 647 channel would be properly aligned even in the case when one of them has very

343 low intensity (e.g. images taken in Vectashield). After alignment both mCherry and AF647 image
344 stacks were cropped to exclude empty space. Same procedure was done for AF488 images.

345 Region of interest for intensity measurements was created by thresholding in mCherry image stack,
346 using Otsu Dark thresholding algorithm. Thresholding was performed in the image that was taken
347 after medium change to exclude cells that were washed away during the change of imaging media.
348 Resulting ROI contained fluorescently labeled nuclei and we refer to it as nuclear ROI. At this point,
349 user intervention was required, to choose ROI that contains no cells, only background noise
350 (background ROI). Afterwards, intensity measurements (mean intensity and integrated density) of
351 nuclear and background ROIs were performed in AF647 and AF488 stacks, respectively.

352 As a result of analysis, macro saved intensity measurement results (in a form of a text file), mCherry
353 before/after image stacks, AF488 or AF647 before/after image stacks and nuclear ROIs.
354 Oversaturated images, poorly aligned images and images where all cells were washed away during
355 imaging media change were excluded from further analysis.

356 Text files with intensity measurement results were imported in Excel and corrected total cell
357 fluorescence (CTCF) was calculated.

358 CTCF = Integrated Density of nuclear ROI – (area of nuclear ROI x mean fluorescence of the
359 background)

360 In addition to CTCF, we calculated average fluorescence by dividing CTCF with the area of nuclear
361 ROI. Calculated values were exported to a separate Excel file for statistical analysis.

362 **Statistical analysis**

363 Statistical analyses (ANOVA and post-hoc analyses) were carried out with IBM SPSS Statistics Version
364 25, Armonk, New York, USA. The power analysis to determine the optimal sample size was carried
365 out with the Statistical Tree Power Calculator, QFAB (Queensland Facility for Advanced
366 Bioinformatics), Brisbane, Australia.

367 **Preparation of data analysis based on pilot work**

368 The dependent variable was the difference (delta) between the fluorescence intensities before and
369 after media change, where the starting medium is always PBS and the change is represented by
370 removing PBS and adding another medium (delta intensity = (intensity PBS – intensity new medium)).
371 Based on prior assumptions, this difference will become minimal in the control condition, where PBS
372 is first removed and the added new medium is again PBS. If another medium is added, delta will be
373 larger and take on an either positive or negative value, depending on whether the intensity in the
374 new medium is smaller or larger than the intensity of PBS.

375 The dependent variable (delta intensity) delivers continuous values and is on interval scale level,
376 which is a prerequisite to carry out an analysis of variance (ANOVA). The independent variables
377 (factors) were different dyes (AF647 and AF488), different imaging media (PBS, Vectashield, 25%
378 Vectashield, GLOX) and different experiments (1, 2 and 3).

379 **Power calculations, randomization and design**

380 Prior to the actual experiments, it was necessary to carry out power calculations to specify the
381 optimal sample size. These analyses needed to take into account multiple analyses, including the
382 different experiments and post-hoc comparisons. Our main focus was to compare delta intensities
383 between different imaging media applying ANOVA. Our defined type 1 error level was 0.05 (including
384 two sided testing for post-hoc, planned comparisons). We aimed for a power of 0.95 (which equals a
385 type 2 error level of 0.05). Based on pilot work, we had estimated to find at least an effect size
386 between 0.45 and 0.5 and more realistic an effect size between 0.8 and 0.9. For the lowest effect of
387 0.45 we would need 23 measurements per condition, for the large effect size of 0.9 we would only
388 need 7 measurements per group to reach the pre-specified power of 0.95. To fulfil the assumptions
389 of ANOVA and post-hoc tests in terms of required distributions, we decided for 20 measurements per
390 condition, which lies within the range of 7 to 23 measurements. We decided in favor of a value at the
391 upper limit of this range because the smaller the sample size, the more likely are violations to the

assumptions of parametric tests such as ANOVA. We did not go beyond this range, though, to avoid having over-powered statistical tests, where tiniest differences would become statistically significant. In our pilot work, we also realized that if images are taken truly at random, a minority of the images could not be measured because no cells appeared after changing media (they got washed away), or some of the images were oversaturated. Because randomization was an absolute requirement for our statistical tests, we needed to have a bigger number than 20 images randomly taken to get a total of 20 measurements. To be safe, we decided a priori that 30 images are taken at random and the first 20 valid images (i.e. those that contained cells before and after media change and that did not contain oversaturated pixels) were included in the analysis. The remaining images were not considered in the analysis. This resulted in the following design:

In each experiment, 20 delta intensities were measured for all 4 different imaging media (20 * 4 = 80). Because they were measured for both dyes, AF647 and AF488, there were 160 delta intensities (80 * 2) per experiment. Because we carried out 3 experiments, there were 480 delta intensities in total (160 * 3).

As a result, there was a 2 (dye) * 4 (imaging media) * 3 (experiment) ANOVA on delta intensities. Following our a priori assumptions, we assumed the two dyes would deliver different delta intensities. In addition, we assumed the 4 imaging media would differ in terms of their delta intensities. Because each experiment took place on a different day with new cells (that were freshly transfected and labeled, etc.), we also expected that the 3 experiments would differ in terms of their delta intensities. In case the 3 experiments indeed differ, different ANOVAs are necessary for each experiment separately, in order to show that the differences between the imaging media point in the same direction and the same post-hoc comparisons are significant in each individual experiment. In these individual ANOVAs, the delta intensities for all imaging media are directly compared to each other for each experiment separately and for each dye separately. Planned post-hoc comparisons (Bonferroni) are subsequently carried out to demonstrate that all post-hoc analyses show the same type of significant differences between the compared imaging media. These planned comparisons

correct the significance levels for multiple tests, i.e. they avoid an accumulation of statistical error which would otherwise occur if multiple significance tests were carried out. To give us maximum trust in our results, we chose the strictest of all post-hoc comparisons, which is the Bonferroni correction. Bonferroni delivers the most conservative results, i.e. the least likely to become statistically significant.

Deriving hypotheses based on prior observations

Based on pilot experiments, our primary focus was dye AF647, because only in AF647 we noticed an intensity drop in image medium Vectashield compared to PBS. We expected that this drop was shown in all 3 experiments. We did not expect such a drop for dye AF488. We do, however, also expect intensity changes on other imaging media for dye AF488. Based on pilot work, we expected medium sized effects relating to a delta intensity increase for Vectashield and 25 % Vectashield. If this increase is robust, it should appear in all three experiments.This also requires planned post-hoc comparisons (Bonferroni), to demonstrate that the significant differences between the compared imaging media are the same for all 3 experiments.

Based on pilot data, we had yet another hypothesis. We realized an intensity drop seen for dye AF647 after adding Vectashield and found out that the intensity will recover after washing. This would be in contrast to the previously assumed dye cleavage effect, where no recovery would be expected. In order to test whether the AF647 intensity drop seen in Vectashield can actually recover, we carried out a repeated measurement ANOVA. In this ANOVA, we compared 3 intensities (1. at PBS baseline, 2. after removing PBS and adding Vectashield, 3. after replacing Vectashield with PBS and waiting 2.5 hours in PBS imaging medium).

Data analyses

In a first step, we carried out a 2 (dye) * 4 (imaging media) * 3 (experiment) ANOVA with the dependent variable delta intensities. There was a significant main effect for dye, $F(1, 456)=819.14$, $p<0.001$, effect size partial $\eta^2=0.64$, Mean AF647=3596.45, Mean AF488=-2569.74,

443 SE(Means)=152.34. Similarly, there was a significant main effect for imaging media, F(3, 456)=424.15,
444 p<0.001, effect size partial η^2=0.74, Mean PBS=420.74, Mean Vectashield=6239.29, Mean_25%
445 Vectashield=-4583.83, Mean GLOX=-22.79, SE(Means)=215.45. In addition, there was a significant
446 main effect for experiment, F(2, 456)=17.58, p<0.001, effect size partial η^2=0.07, Mean expt
447 1=864.28; Mean expt 2=-383.07; Mean expt 3=1058.85, SE(Means)=186.58. Finally, all possible
448 combinations of interactions between the factors were significant, p<0.001. In summary, the delta
449 intensity values differ between dyes, between imaging media, between experiments and the
450 combination of these factors influence each other differently depending on the chosen combination.
451 Consequently, this analysis including all possible factors and their combinations does not permit
452 conclusions, calling for separate ANOVAs in each of the two dyes and separate ANOVAs in each of
453 the 3 experiments. From a biological point of view, it would also not make sense to carry out one
454 ANOVA across both dyes and all conditions.

455 **Separate ANOVA for AF647 in each of the 3 experiments**

456 For dye AF647, there was a main effect for imaging media in all 3 experiments, Experiment 1: F(3,
457 76)=164.46, p<0.001, effect size partial η^2=0.87; Experiment 2: F(3, 76)=182.45, p<0.001, effect size
458 partial η^2=0.88; Experiment 3: F(3, 76)=114.06, p<0.001, effect size partial η^2=82. Looking at the
459 planned, post-hoc comparisons (Bonferroni), the same result was shown in all three experiments:
460 there was a significant (p<0.05) drop of delta intensity from PBS to Vectashield (PBS→VS):
461 Experiment 1 mean delta intensity drop=19348.86, SE(mean intensity drop)=1150.76, Experiment 2
462 mean delta intensity drop=10163.16, SE(mean intensity drop)=564.35, Experiment 3 mean delta
463 intensity drop=13821.93, SE(mean intensity drop=975.89). The other media (25 % Vectashield and
464 GLOX) did not differ significantly from PBS in all 3 experiments, i.e. there was no significant intensity
465 drop. Consequently, the results in all 3 experiments support the notion of an intensity drop only from
466 PBS to Vectashield. This was the result we had expected based on our pilot data. The results are
467 robust because we did not rely on experiment 1 alone, but replicated the results in experiments 2

468 and 3. In all 3 experiments, exactly the same main effects were observed and exactly the same post-
469 hoc comparisons reached statistical significance.

470 **Analysis of AF647 recovery**

471 In addition, we carried out a repeated measures ANOVA to test whether the intensity drop seen in
472 Vectashield can actually recover. We had hypothesized this recovery based on earlier observations
473 we had made in our laboratory when running pilot experiments. Now, we could not rely on delta
474 intensities from 2 measurements, but were rather interested in intensities at 3 different time points.
475 We compared three intensities (1. at PBS baseline, 2. after removing PBS and adding Vectashield, 3.
476 after replacing Vectashield with PBS and waiting for 2.5 hours in PBS imaging medium). We again
477 performed these comparisons for all three experiments separately. In this example, we had a
478 repeated measurement with three consecutive measurements. In this case, the respective analysis
479 depends on a prerequisite for a repeated measurements ANOVA: if sphericity can be assumed based
480 on the Mauchly's Test of Sphericity, no corrections need to be performed. Otherwise, the
481 Greenhouse-Geisser Test of an overall "within subjects effect" with corrected degrees of freedom
482 has to be applied. Because the Mauchly's Test of Sphericity revealed a significant result for all three
483 experiments ($p<0.001$), sphericity could not be assumed and the Greenhouse-Geisser Test was
484 applied for all three experiments. In all three experiments, intensity differences between the 3
485 repeated conditions were statistically significant (1. PBS baseline, 2. after removing PBS and adding
486 Vectashield, 3. after replacing Vectashield with PBS and waiting for 2.5 hours in PBS imaging
487 medium), Experiment 1: $F(1.01, 19.26)=162.68$, $p<0.001$; effect size partial $\eta^2=0.895$; Experiment 2:
488 $F(1.03, 19.48)=175.17$, $p<0.001$, effect size partial $\eta^2=0.9$; Experiment 3: $F(1.18, 22.38)=104.28$,
489 $p<0.001$, effect size partial $\eta^2=0.85$. Given that all three experiments showed a significant overall
490 effect for the repeated conditions, we carried out planned, post-hoc tests with Bonferroni correction
491 to evaluate which of the three time points significantly differed from each other. In each of the three
492 experiments, there was a significant intensity drop from 1. PBS baseline to 2. after removing PBS and
493 adding Vectashield (PBS→VS; in each experiment, $p<0.05$). Similarly, there was a significant recovery

494 from 2. after removing PBS and adding Vectashield to 3. After replacing Vectashield with PBS and
495 waiting for 2.5 hours in PBS imaging medium (VS→PBS:recovery, in each experiment, $p<0.05$). In all
496 three experiments, the recovery was never as strong as to reach the original intensity (in each
497 experiment, $p<0.05$). Consequently, the results demonstrating the recovery effect were very robust.
498 The drop as well as the recovery effect was not only shown in Experiment 1, but replicated exactly in
499 Experiments 2 and 3. In addition, all other post-hoc tests revealed the same results in all three
500 experiments.

501 Detailed results are as follows:

502 Experiment 1 had a PBS baseline intensity mean=24036.37, SE(mean)=1928.87, a drop after
503 removing PBS and adding Vectashield with a mean=3638.06, SE(mean)=359.85, and a recovery after
504 replacing Vectashield with PBS and waiting for 2.5 hours with a mean=16554.7, SE(mean)=1394.89.

505 Experiment 2 had a PBS baseline intensity mean=12270.01, SE(mean)=921.22, a drop after removing
506 PBS and adding Vectashield with a mean=1855.48, SE(mean)=151.16, and a recovery after replacing
507 Vectashield with PBS and waiting for 2.5 hours with a mean=9834.3, SE(mean)=758.21.

508 Experiment 3 had a PBS baseline intensity mean=16984.29, SE(mean)=1589.18, a drop after
509 removing PBS and adding Vectashield with a mean=2376.21, SE(mean)=247.32, and a recovery after
510 replacing Vectashield with PBS and waiting for 2.5 hours with a mean=13369.76,
511 SE(mean)=1367.025.

512 **Separate ANOVA for AF488 in each of the 3 experiments**

513 For dye AF488, there was also a main effect for imaging media in all 3 experiments, Experiment 1:
514 $F(3, 76)=144.36$, $p<0.001$, partial $\eta^2=0.85$; Experiment 2: $F(3, 76)=160.66$, $p<0.001$, partial $\eta^2=0.86$;
515 Experiment 3: $F(3, 76)=101.86$, $p<0.001$, partial $\eta^2=0.8$. Looking at the planned, post-hoc comparisons
516 (Bonferroni), the same result was demonstrated in all three experiments: both Vectashield (PBS→VS)
517 and 25 % Vectashield (PBS→25% VS) showed an increase in delta intensity, which was significantly

518 different from the delta intensity of PBS and GLOX ($p<0.05$), while the delta intensities of PBS and
519 GLOX did not differ significantly from each other. From our pilot work, we had assumed a medium
520 effect size. We did not expect an effect as big as it turned out in our analysis, which came as a
521 surprise to us. The effect was already big in experiment 1 and replicated in experiments 2 and 3. In
522 detail, the results were as follows:

523 In experiment 1, there were no significant delta intensity differences between both PBS imaging
524 media and between PBS and GLOX, but delta intensity showed an increase from PBS to Vectashield
525 with a mean=3906.7 and an increase from PBS to 25 % Vectashield with a mean=9579.34,
526 SE(means)=400.53 (with post-hoc Bonferroni $p<0.05$). The increase was stronger for 25% Vectashield
527 than for Vectashield (with post-hoc Bonferroni $p<0.05$)

528 In experiment 2, there were no significant delta intensity differences between both PBS imaging
529 media and between PBS and GLOX, and delta intensity showed an increase from PBS to Vectashield
530 with a mean=1781.265 and an increase from PBS to 25 % Vectashield with a mean=10930.1,
531 SE(means)=415.99 (with post-hoc Bonferroni $p<0.05$). The increase was once again stronger for 25 %
532 Vectashield than for Vectashield (with post-hoc Bonferroni $p<0.05$).

533 In experiment 3, there were once again no significant delta intensity differences between both PBS
534 imaging media and between PBS and GLOX, and delta intensity showed an increase from PBS to
535 Vectashield with a mean=2297.175 and an increase from PBS to 25 % Vectashield with a
536 mean=3959.1, SE(means)=199.99 (with post-hoc Bonferroni $p<0.05$). The increase was again stronger
537 for 25 % Vectashield than for Vectashield (with post-hoc Bonferroni $p<0.05$).

538

539

540

541

542 **Acknowledgements**

543 This study is supported by the Emmy-Noether programme (project number 317530061 to INS) of the
544 German Research Foundation and the Werner Reichardt Centre for Integrative Neuroscience (CIN) at
545 the Eberhard Karls University of Tübingen. The CIN is an Excellence Cluster funded by the German
546 Research Foundation within the framework of the Excellence Initiative (EXC 307).

547 **Author Contributions**

548 AA, NS and INS performed the experiments and analysis. AA and INS performed dSTORM imaging. RS
549 performed the statistical analysis with the input from INS. INS designed the experiments with
550 statistical advice from RS. INS wrote the manuscript with the input from AA, NS and RS. INS
551 supervised the project.

552 **Competing Interests Statement**

553 The authors declare no competing interests.

554 **References**

555 1 Rust, M. J., Bates, M. & Zhuang, X. Sub-diffraction-limit imaging by stochastic optical
556 reconstruction microscopy (STORM). *Nature methods* **3**, 793-795, doi:10.1038/nmeth929
557 (2006).
558 2 Huang, B., Bates, M. & Zhuang, X. Super-resolution fluorescence microscopy. *Annual review*
559 *of biochemistry* **78**, 993-1016, doi:10.1146/annurev.biochem.77.061906.092014 (2009).
560 3 Heilemann, M., van de Linde, S., Mukherjee, A. & Sauer, M. Super-resolution imaging with
561 small organic fluorophores. *Angewandte Chemie* **48**, 6903-6908,
562 doi:10.1002/anie.200902073 (2009).
563 4 Dempsey, G. T., Vaughan, J. C., Chen, K. H., Bates, M. & Zhuang, X. Evaluation of fluorophores
564 for optimal performance in localization-based super-resolution imaging. *Nature methods* **8**,
565 1027-1036, doi:10.1038/nmeth.1768 (2011).

566 5 Olivier, N., Keller, D., Rajan, V. S., Gonczy, P. & Manley, S. Simple buffers for 3D STORM
567 microscopy. *Biomed Opt Express* **4**, 885-899, doi:10.1364/BOE.4.000885 (2013).
568 6 Cordes, T., Maiser, A., Steinhauer, C., Schermelleh, L. & Tinnefeld, P. Mechanisms and
569 advancement of antifading agents for fluorescence microscopy and single-molecule
570 spectroscopy. *Phys Chem Chem Phys* **13**, 6699-6709, doi:10.1039/c0cp01919d (2011).
571 7 Banterle, N., Bui, K. H., Lemke, E. A. & Beck, M. Fourier ring correlation as a resolution
572 criterion for super-resolution microscopy. *Journal of structural biology*,
573 doi:10.1016/j.jsb.2013.05.004 (2013).
574 8 Huang, B., Wang, W., Bates, M. & Zhuang, X. Three-dimensional super-resolution imaging by
575 stochastic optical reconstruction microscopy. *Science* **319**, 810-813,
576 doi:10.1126/science.1153529 (2008).
577 9 Schindelin, J. *et al.* Fiji: an open-source platform for biological-image analysis. *Nature*
578 *methods* **9**, 676-682, doi:10.1038/nmeth.2019 (2012).
579 10 Linkert, M. *et al.* Metadata matters: access to image data in the real world. *The Journal of cell*
580 *biology* **189**, 777-782, doi:10.1083/jcb.201004104 (2010).
581 11 Thevenaz, P., Ruttimann, U. E. & Unser, M. A pyramid approach to subpixel registration
582 based on intensity. *IEEE Trans Image Process* **7**, 27-41, doi:10.1109/83.650848 (1998).